Interaction of Slow Neutrons with Cobalt and Tin

K. Knopf, W. Waschkowski, A. Aleksejevs[a)], S. Barkanova[a)], and J. Tambergs[a)]

Fakultät für Physik der Technischen Universtität München,
Reaktorstation Garching, D-85747 Garching
[a)] Nuclear Research Center, 31 Miera Str., LV-2169 Salaspils-1, Latvia

Z. Naturforsch. **52 a,** 270–278 (1997); received September 19, 1996

Coherent neutron scattering lengths and total cross sections have been measured on samples of Co, Sn and on isotopically enriched Sn-oxides. The following data were obtained:

- the coherent scattering lengths (in fm) of the bound atoms ^{59}Co (2.49 ± 0.02), ^{nat}Sn (6.22 ± 0.01) ^{116}Sn (6.10 ± 0.01), ^{117}Sn (6.59 ± 0.08), ^{118}Sn (6.23 ± 0.04), ^{119}Sn (6.28 ± 0.03), ^{120}Sn (6.67 ± 0.04), ^{122}Sn (5.93 ± 0.03), and ^{124}Sn(6.15 ± 0.03);
- the thermal absorption cross sections (in b) ^{nat}Sn (0.569 ± 0.005), ^{116}Sn (0.50 ± 0.03), ^{117}Sn (0.77 ± 0.06), ^{118}Sn (0.24 ± 0.06), ^{119}Sn (2.19 ± 0.06), ^{120}Sn (0.55 ± 0.06), ^{122}Sn (0.19 ± 0.06), and ^{124}Sn (0.43 ± 0.06).

New bound levels were evaluated for the investigated nuclei. In combination with the resonance parameters the measured scattering lengths allowed the determination of potential scattering radii R' which are of particular interest for the check of the optical model.

(PACS: 34.50B)

1. Introduction

Neutron scattering lengths and absorption cross sections are important quantities for the interpretation of slow neutrons scattering experiments, which are common methods for fundamental research in physics and other disciplines, for instance for the investigation of the structure and dynamics of condensed matter. In most cases accurate and reliable values are needed as input data not only for elements but also for separated isotopes.

In this paper we report on more exact measurements of coherent scattering lengths $b_{coh}(E_0)$ at almost zero energy E_0 and total cross sections $\sigma_{tot}(E_i)$ at various energies E_i. The scattering lengths and the total cross sections were measured for Co-compounds and for natural Sn and its isotopes. These data form a complete set of input parameters necessary for the evaluation of the nuclear potential scattering radii. This evaluation has fundamental interest for the checking of nuclear optical models. Moreover, new bound levels were fitted, which complete the compiled resonance parameters from [1] and which describe totally the neutron-nucleus interaction over a wide range of neutron energy.

Reprint requests to Dr. W. Waschkowski,
Fax: 089 3209 2162.

2. Basic relations and method of calculations

One of the aims of the present work is the evaluation of the neutron-nucleus strong interaction scattering radii $R'(j)$ for Co and the stable isotopes j of Sn, and the corresponding bound level parameters (resonance energy $E_r(j)$ and neutron width $\Gamma_{nr}(j)$. These parameters were connected with the directly measured values of the neutron total cross sections σ_{tot}^{exp} for natural targets and the bound coherent scattering lengths $b_{coh}(E_0)$ (E_0 = 0.553 meV). The approach in this work is based on the minimization of the difference between the theoretical σ_{tot}^{calc} and experimental σ_{tot}^{exp} neutron transmission cross sections:

$$\sum_i \left[\sigma_{tot}^{calc}(E_i) - \sigma_{tot}^{exp}(E_i)\right]^2 = \min, \qquad (2.1)$$

where the index i assumes the values i = 1, 2, 3, 4 for the monochromatic neutron energies E_i = 1.26, 5.19, 18.6 and 128 eV used in the experiments. The minimization procedure was performed according to

0932-0784 / 97 / 0300-0270 $ 06.00 © – Verlag der Zeitschrift für Naturforschung, D-72072 Tübingen

the Levenberg-Marcardt method of iterations. The measured $\sigma_{\mathrm{tot}}^{\mathrm{exp}}(E_i)$, $b_{\mathrm{coh}}^{\mathrm{exp}}(E_0)$, $\sigma_{\mathrm{abs}}^{\mathrm{exp}}(E_0)$ and some additional data of nuclear resonance parameters found in [1] form the set of input data used in our fit according to (2.1) and to analogous expressions for $b_{\mathrm{coh}}(E_0)$ and $\sigma_{\mathrm{abs}}(E_0)$. The minimum from these expressions do not exceed in most cases of our calculations the square of the mean experimental uncertainty for the corresponding value. The evaluations were carried out for each target separately.

The neutron total cross section $\sigma_{\mathrm{tot}}^{\mathrm{calc}}(E_i)$ for a target can be calculated via the total cross section $\sigma_{\mathrm{tot}}^{\mathrm{calc}}(j, E_i)$ of a certain isotope j and its abundance p_j as

$$\sigma_{\mathrm{tot}}^{\mathrm{calc}}(E_i) = \sum_j \sigma_{\mathrm{tot}}^{\mathrm{calc}}(j, E_i) p_j . \tag{2.2}$$

The total cross section of a separated isotope can be composed as:

$$\begin{aligned}\sigma_{\mathrm{tot}}^{\mathrm{calc}}(j, E_i) = {} & \sigma_{\mathrm{s}}^{\mathrm{calc}}(j, E_i) + \sigma_{\mathrm{abs}}^{\mathrm{calc}}(j, E_i) \\ & + \sigma_{\mathrm{Ls}}^{\mathrm{calc}}(j, E_i) + \sigma_{\mathrm{sol}}^{\mathrm{calc}}(j, E_i),\end{aligned} \tag{2.3}$$

where $\sigma_{\mathrm{s}}^{\mathrm{calc}}(j, E_i)$ is the scattering cross section calculated from the S-matrix formalism, $\sigma_{\mathrm{abs}}(j, E_i)$ the absorption term and $\sigma_{\mathrm{LS}}(j, E_i)$ and $\sigma_{\mathrm{sol}}(j, E_i)$ are small contributions from spin orbital (Schwinger) scattering and solid-state effect cross sections, taken from [2].

At low energies it is quite sufficient to perform calculations only for s-partial wave total cross sections, so $\sigma_{\mathrm{tot}}(j, E_i)$ were taken from [2] as

$$\begin{aligned}\sigma_{\mathrm{sol}}^{\mathrm{calc}}(j, E_i) = \frac{\pi}{k_i^2}\Big(4\sin^2\delta(j, E_i) - 2\sum\nolimits_1 \sin^2\delta(j, E_i) \\ - 4\sum\nolimits_2 \sin^2\delta(j, E_i) + \sum\nolimits_3 + \sum\nolimits_4\Big),\end{aligned} \tag{2.4}$$

where k_i is the neutron wave number and $\delta(j, E_i)$ the total s-wave scattering phase shift, consisting here of strong and neutron electron terms:

$$\begin{aligned}\delta(j, E_i) = -k_i\Big(R'(j) + Z(j) b_{\mathrm{ne}} \frac{A(j)}{A(j) + M_{\mathrm{n}}} \\ \cdot [F(j, E_i) - H(j, E_i)]\Big),\end{aligned} \tag{2.5}$$

where $Z(j)$ and $A(j)$ denote the nuclear charge and the atomic number of isotope j, respectively. The angular averaged atomic formfactor $F(j, E_i)$ and the nuclear charge formfactor $H(j, E_i)$ were taken from [2].

For the neutron-electron scattering length, the numerical value $b_{\mathrm{ne}} = -1.32 \cdot 10^{-3}$ fm, obtained in Garching, was assumed as having the best experimental confirmation (e. g. [3], [4]).

The statistical weighted resonance sums are given as

$$\begin{aligned}\textstyle\sum_1 &= g_+ \textstyle\sum_1^+ + g_- \sum_1^-, \\ \textstyle\sum_2 &= g_+ \textstyle\sum_2^+ + g_- \sum_2^-, \\ \textstyle\sum_3 &= g_+ (\sum_1^+)^2 + g_- (\sum_1^-)^2, \\ \textstyle\sum_4 &= g_+ (\sum_2^+)^2 + g_- (\sum_2^-)^2,\end{aligned} \tag{2.6}$$

where $g_\pm(j)$ denotes the spin statistical factors of the j-th isotope with the nuclear spin $I(j)$:

$$g_+(j) = \frac{I(j) + 1}{2I(j) + 1}, \quad g_-(j) = \frac{I(j)}{2I(j) + 1}. \tag{2.7}$$

At the low energies we are dealing with well resolved resonances, the sums $\sum_1$ and $\sum_2$, can be expressed as

$$\sum\nolimits_1 = \sum\nolimits_{\mathrm{r}}^{\pm} \frac{k_i}{k_{\mathrm{r}}} \frac{\Gamma_{\mathrm{nr}}(E_i - E_{\mathrm{r}})}{(E_i - E_{\mathrm{r}})^2 + \frac{\Gamma_{\mathrm{r}}^2}{4}}, \tag{2.8}$$

$$\sum\nolimits_2 = \sum\nolimits_{\mathrm{r}}^{\pm} \frac{k_i}{k_{\mathrm{r}}} \frac{\Gamma_{\mathrm{nr}}\Gamma_{\mathrm{r}}/2}{(E_i - E_{\mathrm{r}})^2 + \frac{\Gamma_{\mathrm{r}}^2}{4}}. \tag{2.9}$$

The summation in (2.8) and (2.9) must be carried out over all resolved resonance states of the compound nucleus with defined spin value ($\sum^+$ for $J = I + 1/2$ and $\sum^-$ for $J = I - 1/2$) for each isotope j. The resonance energy E_{r}, reduced neutron width $\Gamma_{\mathrm{nr}}^0 = \Gamma_{\mathrm{nr}}/\sqrt{E_{\mathrm{r}}}$, gamma-absorption width $\Gamma_{\gamma\mathrm{r}}$ and compound spin J were inserted in (2.8) and (2.9) as listed in [1]. For the used isotopes it is not necessary to take into account the small contribution of unresolved resonances at high energies. In order to determine the contribution from bound levels (at negative energies), in our case it is possible to combine all bound levels with the same spin state to a single fictive level, defined by a fit.

As the bound coherent scattering lengths were measured at almost zero energy ($E_0 = 0.553$ meV), it is possible to express them via the real part of the total scattering amplitude at the same energy as follows:

$$\mathrm{Re}\, f(j, E_0) = -b_{\mathrm{coh}}^{\mathrm{calc}}(j, E_0) \frac{A(j)}{A(j) + M_{\mathrm{n}}}, \tag{2.10}$$

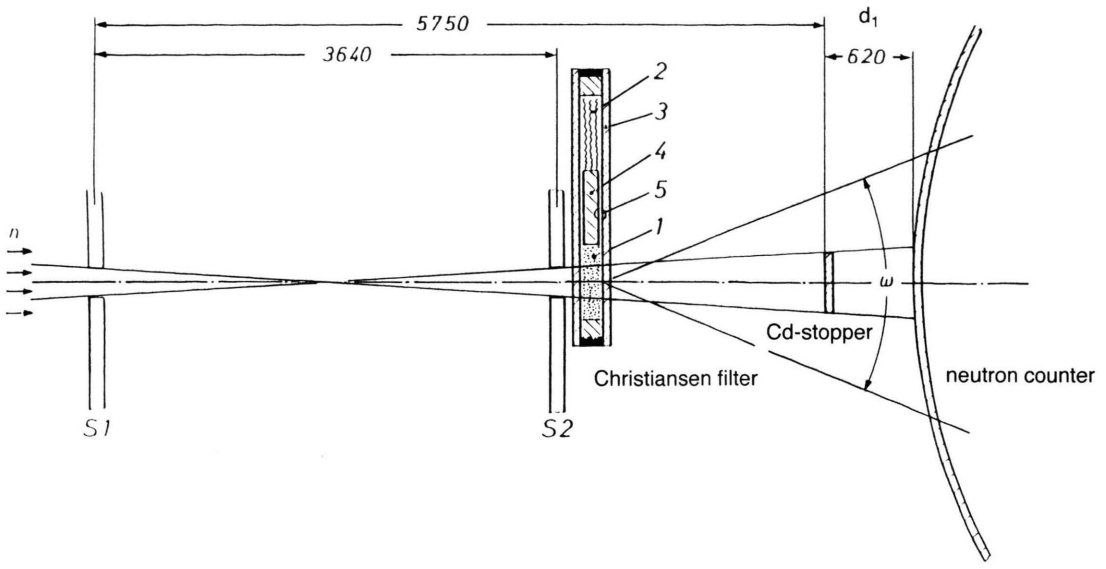

Fig. 1. Experimental set-up for Christiansen filter- and total cross section measurements; slits S_1 and S_2: 0.4 mm for Christiansen filter, Cd-stopper: 1.0 mm; 1 powder, 2 liquid, 3 glass, 4 distance holder, 5 liquid slits; d_1 distance for total cross section measurements (SnO_2).

where

$$\begin{aligned}\mathrm{Re}\, f(j, E_0) = {} & g_+(j)\mathrm{Re}\, f^+(j, E_0) \\ & + g_-(j)\mathrm{Re}\, f^-(j, E_0)\end{aligned} \tag{2.11}$$

and Re $f^{\pm}(j, E_0)$ is according to [2] given as

$$\begin{aligned}\mathrm{Re}\, f^{\pm}(j, E_0) = \frac{1}{2k_0}\big((1 - \textstyle\sum_2^{\pm})\sin 2\delta(j, E_0) \\ - \textstyle\sum_1^{\pm}\cos 2\delta(j, E_0)\big).\end{aligned} \tag{2.12}$$

From (2.10) the already mentioned condition for the minimization procedure can be deduced:

$$\sum_j \left[\frac{A(j) + M_n}{A(j)}\mathrm{Re}\, f(j, E_0) + b_{\mathrm{coh}}^{\mathrm{exp}}(j, E_0)\right]^2 = \min, \tag{2.13}$$

$$\sigma_{\mathrm{abs}}^{\mathrm{calc}}(j, E_0) = g_+\sigma_{\mathrm{abs}}^{\mathrm{calc}}(j, E_0)^+ + g_-\sigma_{\mathrm{abs}}^{\mathrm{calc}}(j, E_0)^-, \tag{2.14}$$

where

$$\sigma_{\mathrm{abs}}^{\mathrm{calc}}(j, E_0)^{\pm} = \pi \textstyle\sum_r^{\pm} \dfrac{1}{k_r k_0} \dfrac{\Gamma_{\mathrm{nr}}\Gamma_{\gamma r}}{(E_0 - E_r)^2 + \frac{\Gamma_r^2}{4}}, \tag{2.15}$$

k_r and k_0 are the neutron wave numbers at the energies E_r and E_0.

In this case the bound level parameters must also satisfy the equation for absorption:

$$\sum_j \left[\sigma_{\mathrm{abs}}^{\mathrm{calc}}(j, E_0) - \sigma_{\mathrm{abs}}^{\mathrm{exp}}(j, E_0)\right]^2 = \min. \tag{2.16}$$

The simultaneous minimizations of (2.1), (2.13) and (2.16) have given the values of $\sigma_{\mathrm{tot}}^{\mathrm{calc}}(E_i)$, $\sigma_{\mathrm{abs}}^{\mathrm{calc}}(j, E_i)$ and $b_{\mathrm{coh}}^{\mathrm{calc}}(j, E_i)$, and this set is in very good agreement with the corresponding measured values. Therefore the strong interaction scattering radii $R'(j)$ and the bound level parameters $E_r(j)$ and $\Gamma_{\mathrm{nr}}(j)$, evaluated for each isotope from this input set, can be considered as rather reliable.

3. Experiment

3.1. Methods

All measurements were performed at the FRM reactor (open pool, 4 MW thermal power) of the Technical Universtiy of Munich. Coherent scattering lengths were measured using the Christiansen filter technique in a small angle scattering device which works with very slow neutrons of mean energy 0.553 meV. Figure 1 shows the experimental set-up. The filter consisted of a homogeneous mixture of a powder

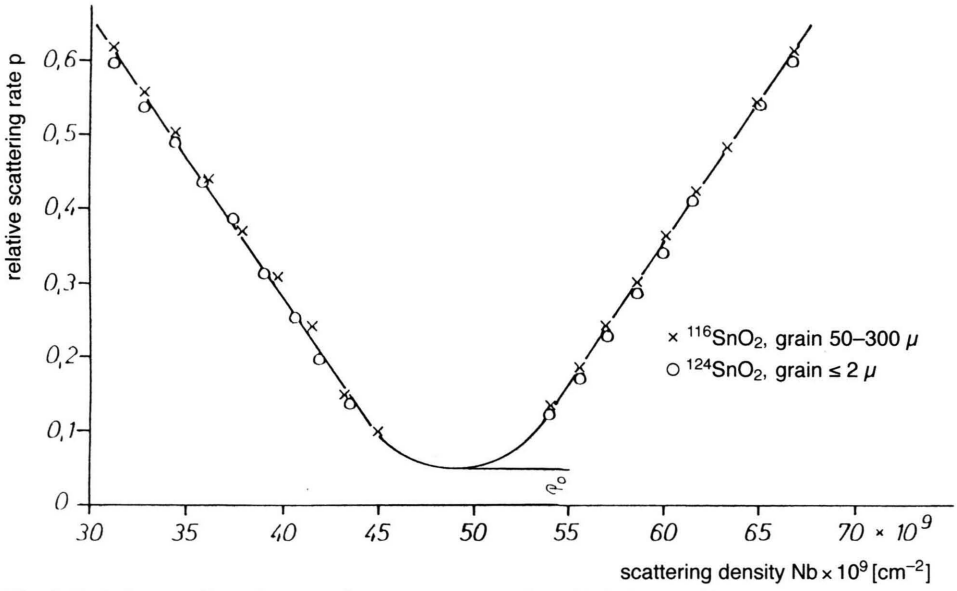

Fig. 2. Relative small angle scattering rates measured on Christiansen filters.

sample and a mixture of the following liquids with well known scattering densities Nb in 10^9 cm^{-2}: C_6H_6 [11.819(6)], C_2Cl_4 [30.412(4)], C_6D_6 [100% D: 54.31(3)] and C_6D_{12}[100% D: 67.06(4)]. The densities D for 100 atom % are $D(C_6D_6) = 0.94945(5)$ g/cm^3 and $D(C_6D_{12}) = 0.89334(1)$ g/cm^3.

When the scattering densities of the powder $(N\bar{b})_p$ and that of a mixture of liquids $(N\bar{b})_L$ became equal, the small angle scattering vanished totally, except a small residual scattering rate p_0, which can be explained by some inhomogeneities from grain to grain. The residual has nearly no influence on the accuracy of the balance scattering density. In detail the experimental technique is described in [5], and the revised data handling in [6].

Two typical scattering curves are presented in Fig. 2 as small-angle scattering rates versus scattering density of the liquid fillings. The physical data of the powder samples and the measured coherent scattering lengths at energy E_0 are compiled in Table 1 for Co-compounds and the natural SnO_2-oxides and in Table 2 for the isotopically enriched SnO_2-oxides.

Total transmission cross sections σ_{tot}^{exp} were determined using the slow neutrons of the same small angle scattering device for transmission measurements on solid or powdered samples. In this case the small angle scattering from the target was eliminated by a special arrangement of the target at a position from which all forward scattered neutrons hit the neutron detector (for details see [7]).

The energy selectivity was obtained by quasi-continuously working resonance activation detectors (Rh at 1.26 eV; Ag at 5.19 eV). For a description of this technique and the data reduction process we refer to [8].

The mono-energetic neutrons of 18.6 eV and 128 eV were separated in a tangential tube by resonance scattering on targets of W- and Co-foils, respectively (see [9]).

3.2. Substances

The Christiansen filter measurements required crystalline powder samples of natural or isotopically enriched compounds. Compounds had to be taken, because metallic powders may have an undefined oxidation. The sample densities were measured pycnometrically with C_2Cl_4 and C_7H_8 as reference liquids. The density values given in Table 1 for SnO_2-I/II (D = 6.983(5) g/cm^3 in C_2Cl_4 and D = 6.990(7) g/cm^3 in C_7H_8) correspond to the tetragonal crystal form with D = 6.992(11) g/cm^3 at 293 K [10]. The density D = 6.915(12) g/cm^3 for SnO_2-III complies with another crystal modification, which can exist after [11] as a high temperature phase or as amorphous.

The densities of the isotopically enriched SnO_2, listed in Table 2, agree well with the data deduced

Table 1. Physical data of Co-compound and natural Sn-oxides and results of Christiansen filter measurements.

Sample	Modification [a]	Drying [b] K	D (lit.) [a] g·cm^{-3}	D (pyk.) g·cm^{-3}	p_0 [c]	Nb 10^9·cm^{-2}	b (mol) fm	b (atom) fm
$CoCl_2$	trigonal or	570(N)	3.356	3.393(6)	0.04	34.03(5)	21.62(5)	
	rhombic	500(A)		3.357(1)	0.005	33.71(7)	21.65(4)	
		420(A)		3.355(19)	0.005	33.58(9)	21.59(6)	
						mean value:	21.62(3)	2.462(30)
$CoSO_4$	orthorhombic	720(O)	3.71	3.766(4)	0.05	40.77(8)	28.54(7)	
		770(N)		3.566(9)	0.15	39.60(5)	28.58(8)	
						mean value:	28.56(6)	2.467(60)
CoF_2-I	tetragonal	660(A)	4.46	4.273(22)	0.04	26.60(4)	13.79(8)	
CoF_2-II		670(V)		4.478(6)	0.03	38.32(4)	13.77(2)	
						mean value:	13.78(4)	2.488(50)
CoO	kubic	1270(N)	6.438(9)	6.418(3)	0.06	42.96(5)	8.33(1)	
		1220(Ar)		6.370(8)	0.13	42.52(4)	8.31(1)	
CoO[d]		orig.		6.423(13)	0.03	42.89(3)	8.31(1)	
		960(Ar)		6.386(28)	0.20	42.62(5)	8.30(4)	
						mean value:	8.315(9)	2.510(10)
$CoTiO_3$	hex-R	870(A)	4.986(3)	4.893(6)	0.12	31.53(5)	16.57(1)	
		1070(A)		4.895(2)	0.12	31.58(6)	16.59(3)	
						mean value:	16.58(1)	2.518(25)
							mean value Co:	**2.489(16)**
SnO_2-I	tetragonal	680(A)	6.996(11)	6.997(8)	0.053	49.85(6)	17.83(3)	
		1270(A)		6.997(8)	0.030	49.89(3)	17.84(2)	
						mean value:	17.83(2)	6.223(21)
SnO_2-II	tetragonal	orig.		6.987(8)	0.029	49.79(4)	17.83(3)	
		bg.		6.987(8)	0.045	49.79(4)	17.83(3)	
		680(A)		6.987(4)	0.039	49.83(50)	17.85(3)	
		870(A)		6.987(4)	0.033	49.92(5)	17.88(3)	
		1270(A)		6.987(4)	0.016	49.77(6)	17.82(3)	
						mean value:	17.84(1)	6.231(16)
SnO-III	hex. or rhomb.	bg.		6.917(13)	0.023	49.23(13)	17.81(6)	
				6.913(21)	0.037	49.19(4)	17.81(6)	
				6.994(10)	0.027	49.82(7)	17.82(4)	
						mean value:	17.81(3)	6.202(31)
							mean value Sn:	**6.219(13)**

[a] Ref. [10]; [b] different drying: (orig.) = original powder, (N) = Nitrogen, (O) = oxigen, (Ar) = argon, (A) = air, (V) = vacuum; [c] p_0 = small residual scattering rate from sample inhomogeneties; [d] powdered single crystal from Kischko [16].

from the density of ordinary SnO_2-III. In order to improve the accuracy of the transmission measurements, metallic Co- and Sn-targets of high purity were used. Their measured densities (D(Sn) = 7.287(2) g/cm^3 and D(Co) = 8.821(2) g/cm^3 at 293 K) are in sufficient agreement with data from the literature (D(Sn) = 7.287(3) g/cm^3 and D(Co) = 8.9 g/cm^3 [11]).

4. Results

4.1. Scattering Lengths

The obtained coherent scattering lengths of the bound atoms are listed for the natural elements in the last column of Table 1 and for the separated Sn-isotopes in Table 3. For the deduction the following scattering lengths of the compound elements were used:

$b(0)$ = 5.805(4) fm [12], b(F) = 5.654(12) fm [12], b(Cl) = 9.5792(8) fm [13], b(S) = 2.847(1) fm [14], b(Ti) = –3.370(13) fm [15].

The average values of the scattering lengths in comparison with the literature are as follows:

Co: The obtained b(Co) = 2.49(2) fm agrees well with the value b(Co) = 2.53(5) fm [16] from neutron interferometry and also with b(Co) = 2.50(3) fm [17] deduced from earlier Christiansen filter measurements without any water corrections.

Table 2. Physical data on istopically enriched SnO_2-samples and results from Christiansen filter measurements.

Iso.	Purity %	Grain μm	Drying[a] K	Density (pyk.) g·cm^{-3}	p_0 [b]	Nb 10^9·cm^{-2}	b (mol) fm	b (atom) fm
Sn-116	99.89	50 - 300	870	6.844(28)	0.047	49.01(7)	17.75(5)	6.14(5)
			1270	6.844(28)	0.060	48.83(11)	17.69(6)	6.08(6)
Sn-117	99.85	50 - 300	870	6.866(31)	0.030	50.36(9)	18.24(5)	6.63(5)
			1270	6.866(31)	0.029	49.96(7)	18.09(5)	6.48(5)
Sn-118	99.90	≤ 2	870	6.937(20)	0.085	49.34(5)	17.87(4)	6.26(4)
			1270	6.937(20)	0.088	49.22(6)	17.83(4)	6.22(4)
Sn-119	99.94	5-50	1270	6.909(34)	0.039	49.46(3)	17.91(4)	6.30(4)
			1270	6.909(34)	0.028	49.36(12)	17.87(6)	6.26(6)
Sn-120	99.91	≤ 2	1270	7.004(37)	0.106	50.44(8)	18.27(5)	6.66(5)
			1270	7.004(37)	0.039	50.46(5)	18.28(4)	6.67(4)
Sn-122	99.87	≤ 2	1270	7.085(30)	0.10	48.42(5)	17.54(4)	5.93(4)
			1270	7.085(30)	0.11	48.51(8)	17.57(5)	5.96(5)
Sn-124	99.94	≤ 2	1270	7.155(14)	0.051	49.03(4)	17.76(2)	6.15(2)
			1270	7.155(14)	0.039	49.06(9)	17.77(4)	6.16(4)

[a] all samples are dried in air; [b] p_0 = small residual scattering rate from sample inhomogeneities.

Table 3. Isotopic abudances of enriched SnO_2-samples and deduction of scattering lengths for separated isotopes.

		Sn-sample enriched in mass A isotope						
A	nat	116	117	118	119	120	122	124
112	0.010	0.0003	< 0.0005	< 0.0001	< 0.001	< 0.0002	< 0.0010	< 0.0004
114	0.007	0.0001	< 0.0002	< 0.0001	< 0.0005	< 0.0002	< 0.0006	< 0.0002
115	0.004	0.0005	< 0.0001	< 0.0001	< 0.0005	< 0.0002	0.0010	< 0.0004
116	0.147	0.963(2)	0.0135	0.0009	< 0.0005	0.0003	0.0032	0.0018
117	0.077	0.0126	0.918(4)	0.0040	< 0.0005	0.0002	0.0012	0.0011
118	0.243	0.0161	0.0530	0.979(2)	0.097	0.0011	0.0079	0.0050
119	0.086	0.0019	0.0062	0.0083	0.891(5)	0.0022	0.0028	0.0029
120	0.324	0.0042	0.0079	0.0069	0.0106	0.995	0.0238	0.0134
122	0.046	0.0007	0.0006	0.0003	0.0005	0.0008	0.953(3)	0.0018
124	0.056	0.0004	0.0008	0.0006	0.0005	0.0002	0.0081	0.974
b(at)[a] [fm]		6.11(4)	6.56(8)	6.24(3)	6.28(4)	6.67(3)	5.95(3)	6.16(3)
b(is) [fm]	6.24(4)	6.10(1)	6.59(8)	6.23(4)	6.28(3)	6.67(4)	5.93(3)	6.15(3)
Lit. [21]	—	5.8(1)	6.4(3)	5.8(1)	6.0(3)	6.4(1)	5.5(3)	5.9(2)

[a] b(at) = scattering lengths of the isotope mixtures of the enriched samples; b(is) = scattering lengths of the separated isotope.

Table 4. Transmission measurements with very slow neutrons on solid natural Sn-samples.

Samples	Thickness cm	Slit 1 mm	Wavelength Å	Pos.[a] cm	$\sigma_{tot}(E_0)$ b	$\sigma_{inel}(E_0)$ b	$\sigma_{abs}(E_0)$[b] b	σ_{abs} (0.0253eV) b
solid-I	3.5358(8)	1.5	12.1(1)	62	4.13(2)	0.33(1)	3.79(7)	0.563(11)
		1.5	12.0(1)	270	4.17(5)	0.32(1)	3.84(6)	0.575(11)
solid-II	3.8390(9)	1.5	12.1(1)	62	4.18(3)	0.33(1)	3.84(4)	0.570(8)
		1.5	12.1(1)	270	4.19(3)	0.33(1)	3.85(4)	0.572(8)
solid- III	4.7853(9)	0.4	11.5(1)	62	4.01(5)	0.31(1)	3.69(6)	0.577(11)
		0.4	12.4(1)	62	4.20(5)	0.33(1)	3.86(6)	0.559(10)
							mean value Sn:	**0.569(5)**

[a] Pos. = distance between sample and counter;
[b] evaluation with Debye-temperature Θ_D = 187(12) K and incoherence $\sigma_i(E_0)$ = 0.01(1) b.

Table 5. Transimssion measurements with very slow neutrons on natural and enriched SnO_2-samples.

Sample	Grain of the powder	Drying[a] K	Slit 1 mm		$\sigma_{tot}(E_o)$ [b] b	σ_{inel} b	Θ_D K	$\sigma_{abs}(E_{th})$ [c] b
nat. powder-I	≤ 2	680	1.5		7.2(3)			
		1270	1.5		7.5(2)			
				mean value:	**7.4(2)**	**3.6(2)**	**220(20)**	**3.7(3)**
nat powder-II	100	orig.	1.5		6.6(5)			
	50	pb.	1.5		6.5(5)			
				mean value:	**6.6(4)**	**2.7(4)**	**320(5)**	**3.8(6)**
	50	680	1.5		5.6(4)			
	50	870	1.5		6.4(3)			
	50	1270	1.5		5.7(5)			
				mean value:	**5.9(3)**	**2.1(2)**	**400(40)**	**3.7(4)**
nat powder-III	30	pb.	1.5		9.0(4)	5.2(4)	130(20)	3.7(4)
	30	680	1.5		6.9(2)			
	30	1270	1.5		7.5(8)			
				mean value:	**7.2(4)**	**3.3(4)**	**250(40)**	**3.8(6)**
Sn-116	50-300	1270	0.4		8.0(7)			
Sn-117	50-300	1270	0.4		9.6(3)			
Sn-118	≤ 2	1270	0.4		6.3(2)			
Sn-119	5-50	1270	0.4		18.0(6)			
Sn-120	≤ 2	1270	0.4		8.3(2)			
Sn-122	≤ 2	1270	0.4		6.0(2)			
Sn-124	≤ 2	1270	0.4		7.5(3)			
				$\sum p_j \sigma_j =$	**8.5(3)**	**4.6(3)**	**160(20)**	**3.8(4)**

[a] different drying: (org.) original powder, (pb.) powdered in ball grinder. All other samples are dried in air;
[b] $E_0 = 0.553$ meV; [c] $E_{th} = 0.0253$ eV.

Table 6. Deduction of absorption cross sections from transmission measurements at 0.553 meV on enriched SnO_2 and comparison with literature and calculation (cross sections in barns).

	From mesurements					Ref. [1]	From calculation	
A	$\sigma_{tot}(E_0)$	σ_{inel}	$\sigma_{inc}(sp)$	$\sigma_{abs}(E_0)$	σ_{abs} (0.0253 eV)	σ_{abs} (0.0253 eV)	σ_{abs} [a] (0.0253 eV, res. par.)	$\sigma_{abs}(E_0)$ [b] (new fit bound level)
116	8.0(7)	4.6(3)		3.4(8)	0.50(3)	0.14(3)	0.12(1)	3.39(60)
117	9.8(3)	4.6(3)	0.009(10)	5.2(4)	0.77(6)	2.3(5)	2.16(4)	5.19(30)
118	6.2(2)	4.6(3)		1.6(4)	0.24(6)	0.22(5)	0.175(2)	1.59(30)
119	19.4(2)	4.6(3)	0.001(10)	14.8(4)	2.19(6)	2.2(5)	2.18(2)	14.79(30)
120	8.3(2)	4.6(3)		3.7(4)	0.55(6)	0.14(3)	0.17(1)	3.69(30)
122	5.9(2)	4.6(3)		1.3(4)	0.19(6)	0.18(2)	0.16(1)	1.29(30)
124	7.5(3)	4.6(3)		2.9(4)	0.43(6)	0.13(1)	0.14(1)	2.89(30)
				$\sum p_j \sigma_j =$	**0.59(5)**	**0.50(11)**	**0.48(1)**	

[a] with resonance parameters from [1];
[b] with the same resonance parameters but new bound level fits.

From new bound level fits, being compiled in Table 8, the spin state scattering lengths $b_\pm$ were calculated and resulted in $b_+ - b_- = -12.79(5)$ fm, which is more accurate than the literature value and can be compared with the directly measured $b_+ - b_- = -12.5(4)$ fm (Glättli [19]) and with $-13.8(5)$ fm (Schermer [20]). The spin state scattering lengths lead to a bound spin incoherent cross section of $\sigma_{inc}(sp) = 5.06(2)$ b, which is consistent with $\sigma_{inc}(sp) = 5.04(8)$ b from [1].

Sn: For natural tin, $b(Sn) = 6.22(1)$ fm was obtained, which agrees well with the very precise gravity refractometer value $b(Sn) = 6.225(2)$ fm [18]. The results on enriched SnO_2-samples are shown in Table 2, from which the coherent scattering lengths of the single isotopes are deduced in Table 3. They are much

Table 7. Total cross sections of metallic Co- and Sn-samples.

		Co		Sn			
E_i	eV	1.26	5.19	1.26	5.19	18.6	128
$\sigma_{tot,meas}$	b	11.23(4)	8.68(8)	5.032(6)	4.922(4)	5.046(25)	5.321(12)
$\sigma_{tot,calc}$	b	11.23(3)	8.73(8)	5.048(7)	5.004(4)	5.039(20)	5.321(10)

Table 8. New bound level fits for Co- and Sn-isotopes and obtained potential radii R' (values in parenthesis are from [1]).

	Bound level parameters							Obtained data				
Sample	E_r eV		J	$\Gamma_{\gamma,r}$ meV	$h^{a)}$	$hg\Gamma_r^0$ meV		R' fm	b_+ fm	b_- fm	b_{calc} fm	b_{exp} fm
^{59}Co	–387	(–500)	3	447	2	106	(1868)	6.10(5)	–9.21	3.58	2.49	2.49(2)
	–481	(–475)	4	447		1700	(130.3)					
^{116}Sn	–61.9	(—)	0.5	52	1	5.97	(6.4)	6.22(5)	–0.19	—	6.08	6.10(1)
^{117}Sn	–52.7	(–29.2)	1.0	78	2	10.81	(11.1)	6.31(5)	+0.220	–0.227	6.58	6.59(8)
	–96.3	(—)	0	78		5.32	(—)					
^{118}Sn	–86.8	(–100)	0.5	88	1	4.94	(4.1)	6.31(5)	–0.16	—	6.20	6.23(4)
^{119}Sn	–9.92	(–10)	1.0	87	2	1.21	(1.2)	6.12(5)	+0.137	0.000	6.27	6.28(3)
	—	(—)	0			—	(—)					
^{120}Sn	–365	(–612)	0.5	76	1	233	(200)	5.48(5)	+1.09	—	6.62	6.67(4)
^{122}Sn	–7.69	(–10)	0.5	85	1	0.033	(0.039)	6.07(5)	–0.20	—	5.92	5.93(3)
^{124}Sn	–12.1	(–20)	0.5	87	1	0.177	(0.15)	6.09(5)	+0.01	—	6.14	6.15(3)

[a)] factor with which the reduced scattering width is multiplied.

more accurate than old values being deduced from Bragg diffraction [21] (last row of Table 3). Weighted with the abundance, the isotopic scattering lengths lead to $b(\mathrm{Sn}) = 6.24(4)$ fm, being in good agreement with the directly measured and above mentioned value for natural Sn.

The isotopic scattering lengths lead to an isotope incoherence according to $\sigma_{inc}(\mathrm{is}) = 2\pi \sum_{k,l} p_k p_l (b_k - b_l)^2$ of $\sigma_{inc}(\mathrm{is}) = 0.007(14)$ b. The spin incoherence comes from the isotopes ^{117}Sn and ^{119}Sn; the new bound level fits (see Table 8) result in a spin incoherence of $\sigma_{inc}(\mathrm{sp}) = 0.001(1)$ b for natural Sn, so that the total incoherence becomes $\sigma_{inc} = 0.008(14)$ b, which can be compared with $\sigma_{inc} = 0.022(5)$ b from [1].

4.2. Total Cross Sections

The results of total cross section measurements at $E_0 = 0.553$ meV are compiled for metallic Sn-samples in Table 4 and for natural and enriched Sn-oxides in Table 5. The average value for natural Sn at thermal neutron energy (using the $1/\sqrt{E}$ law for the small extrapolation) in solids becomes $\sigma_\gamma = 0.569(5)$ b and agrees well with powders $\sigma_\gamma = 0.550(30)$ b. The reason for the different value to $\sigma_\gamma = 0.626(9)$ b in [1] is unknown.

The absorptions of the single isotopes are given in Table 6; weighted with the abundance, they lead for natural Sn to $\sigma_\gamma = 0.59(5)$ b. Because of the big standard deviation, that value agrees with corresponding other values. The absorption, being calculated with the new bound level fit of Table 8, is practically identical with the measured ones, as shown in the last column of Table 6 for each isotope.

The results of total cross section measurements in the eV-energy region on metallic samples are compiled in Table 7. (The available quantities of enriched samples were not big enough for such transmission measurements.) The S-matrix calculations using the bound level fits reproduce the measured total cross sections at the energies E_i very well, supprisingly even in case of $E_i = 128$ eV for Sn which has several resonances close by. A small difference at 5.19 eV is explainable by the experimental technique implying an overlap of secondary resonance effects of the used silver detector with resonances of Sn.

4.3. Bound Level Parameters

The sets of bound level fits obtained from the minimization of (2.1), (2.13) and (2.16), are compiled in Table 8. These fits describe completely and consistently all parameters of the low energy interaction of neutrons with the concerned nuclei.

In some cases the new bound levels differ remarkably from the data in [1], which are also presented in Table 8 in parenthesis.

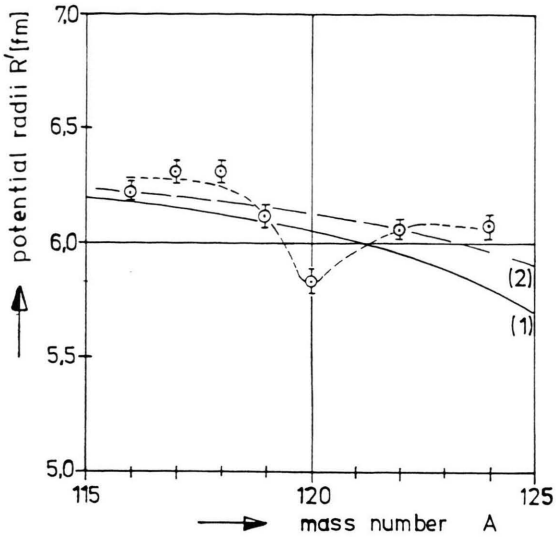

Fig. 3. Mass dependence of the potential radii, (1) from optical model calculation on deformed nuclei, (2) from optical model calculation on spherical nuclei.

4.4. Potential Radii

The relation between the obtained potential radii of strong interaction $R'(j)$ and the mass number $A(j)$ is shown in Figure 3. The values lie very close to the prediction of optical model curve being transfered from [1] into that graph, except R' obtained for $A(j) = 120$. This finding is not surprising; it can be explained by the effect of closed shells in nuclei. This idea will be the subject of a future investigation over a more expanded mass region for a more realistic optical model which takes account of the nuclear size dip at magic numbers.

5. Conclusion

The measurements, presented in this paper, give more accurate data to describe the interaction of slow neutrons with Cobalt and Tin and it's isotopes in the region from zero up to eV energies. The new data sets became homogenious and consistent by new bound level fits which allowed a rather exact determination of the difference between statistically weighted total lengths $b_+(j, E_0) - b_-(j, E_0)$ and the nuclear potential scattering radii $R'(j)$. This finding makes the data sets very reliable. The set of parameters such as evaluated in the present work, but for a wider mass region, would give a possibility to design a very realistic optical potential.

Acknowledgements

The financial support of the "Bundesministerium für Forschung und Technologie" is appreciated. The Latvian group are thankful for the financial support from the German Vorlkswagen-Stiftung. Also many thanks to the reactor staff for continuous assistance.

[1] S. F. Mughabghab, M. Divadeenam, and N. E. Holden, Neutron Cross Section Vol. **I A**, Academic Press , New York 1981.
[2] S. Barkanova, M. Sc. degree diploma work, Riga 1996, unpublished.
[3] L. Koester, W. Waschkowski, and J. Meier, Z. Phys. A **329**, 229 (1988).
[4] Koester, W. Waschkowski, L. V. Mitsyna, G. S. Samosvat, P. Prokofjevs, and J. Tambergs, Phys. Rev. C **51**, 3363 (1995).
[5] L. Koester and K. Knopf, Z. Naturforsch. **26a**, 391 (1971).
[6] L. Koester and K. Knopf, Z. Phys. A **338**, 233 (1991).
[7] K. Knopf and W. Waschkowski, J. Neutron Reasearch, accepted
[8] W .Waschkowski and L. Koester, Z. Naturforsch. **31a**, 115 (1976).
[9] W. Dilg and H. Vonach, Nucl. Instr. Meth. **100**, 82 (1972).
[10] Handbook of Chemistry and Physics 67th Ed. CRC Press, Inc. Boca Raton, Florida 1986.
[11] Gmelins Handbuch der organischen Chemie, Sys. Nr. **46**, Verlag Chemie, Weinheim 1972.
[12] L. Koester, K. Knopf, and W. Waschkowski, Z. Phys. A **292**, 95 (1979).
[13] L. Koester and W. Nistler, Z. Phys. A **292**, 95 (1979).
[14] W. D. Trüstedt, Z. Naturforsch. **26a**, 400 (1971).
[15] L. Koester, K. Knopf, and W. Waschkowski, Z. Phys. A **345**, 175 (1993).
[16] U. Kischko, J. Schweizer, and F. Tasset, Z. Phys. A **307**, 163 (1982).
[17] L. Koester, K. Knopf, and W. Waschkowski, Z. Phys. **271**, 201 (1974).
[18] G. Reiner, W. Waschkowski, and L. Koester, Z. Phys. A **337**, 221 (1990).
[19] H. Glättli, G. L. Bachella, M. Fourmond, A. Malinowski, P. Meriel, M. Pinot, P. Roubeau, and A. Abragam, J. Phys. (Paris) **40**, 629 (1979).
[20] R. J. Schermer, Phys. Rev. A **135**, 584 (1965).
[21] A. Kay, J. Acta Cryst. **23**, 868 (1967).